This is an open access article published under a Creative Commons Attribution (CC-BY) License, which permits unrestricted use, distribution and reproduction in any medium, provided the author and source are cited.

ACS AUTHORCHOICE

ACS Sustainable Chemistry & Engineering

pubs.acs.org/journal/ascecg

Research Article

Lignin–Zein Composite: Synthesis, Three-Dimensional Printing, and Microbial Degradation

Jin Gyun Lee,[‖] Yusheng Guo,[‖] Jorge A. Belgodere, Ahmed Al Harraq, Aubry A. Hymel, Amber J. Pete, Kalliat T. Valsaraj, Michael G. Benton, Mary G. Miller, Jangwook P. Jung, and Bhuvnesh Bharti*

Cite This: *ACS Sustainable Chem. Eng.* 2021, 9, 1781–1789

Read Online

ACCESS | Metrics & More | Article Recommendations | Supporting Information

ABSTRACT: Worldwide use and disposal of plastics have reached a dramatic saturation point, polluting lands, oceans, and air across the globe. Responding to such a challenge requires, among other environmental remediation measures, the manufacture of alternative sustainable plastics. Recent studies in the area have enabled the development of degradable plastics; however, the rate and conditions required for the degradation of such materials remains under scrutiny. Here, we introduce a new class of fully plant-based, rapidly degradable lignin and zein composite blend that can be transformed into macroscopic structures using extrusion three-dimensional (3D) printing. Corn-derived zein forms the polymeric solution, while insoluble lignin granules act as a binder for enhanced printability and facile degradation. The blend showcases a shear-thinning behavior that is ideal for rapid extrusion printing into desired 3D structures, from cuvette caps to circuit boards. Biodegradation studies show that common bacteria readily found in soil and compost are able to decompose structures made with the lignin–zein composite in shorter time frames compared to a known biodegradable plastic, viz., polylactic acid. The rapid biodegradability and enhanced processability highlight the potential of lignin–zein composites to decrease our dependence on petroleum oil-based plastics.

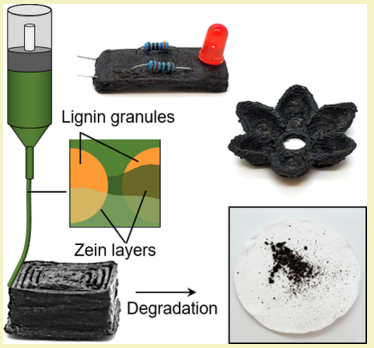

KEYWORDS: *additive manufacturing, biodegradable composite, sustainable materials, plant-based materials, bio-based plastics*

Downloaded via Bhuvnesh Bharti on February 4, 2021 at 14:09:09 (UTC).
See https://pubs.acs.org/sharingguidelines for options on how to legitimately share published articles.

INTRODUCTION

Plastics are the backbone of modern manufacturing with 8300 million metric tons produced worldwide from 1950 to 2015.[1] However, only 9% of plastic in the world is recycled, and the vast majority is simply discarded into the environment after use.[1,2] Most plastics are synthesized using petroleum oil and, when discarded in nature, do not decompose readily and are expected to persist even at geological timescales.[3] Recent studies have found that synthetic plastics released into the environment can break up into microscopic fragments called microplastics.[4] These microplastics seem to be omnipresent and undesirably integrated into the food chain, thus posing great danger to living organisms.[5−8] Thus, there is an immediate need for sustainable alternatives to eliminate our reliance on traditional plastics.[9]

Recent trends in the development of sustainable manufacturing have pointed toward plant-based, biodegradable materials as precursors to move society toward a more circular economy.[10−13] Such materials should be designed to be sourced with biomass that is renewable and decentralized and to be destined for biodegradation into small molecules at the end of their lifecycle.[14,15] For example, polylactic acid (PLA) has garnered considerable attention as a biodegradable alternative in the packaging industry.[16] Despite its reputation, PLA shows no significant degradation in artificial sea and fresh water.[17,18] PLA-based materials require bio-augmented soils with specific microbial characteristics for complete degradation.[19] To address the challenge of material sustainability, alternatives should be derived from naturally occurring precursors that can be produced inexpensively at a large scale with low carbon impact.[20] Concurrently, these materials must rapidly decompose upon release into the environment. Here, we introduce a new class of a lignin–zein composite (LZC) that can be processed into macroscopic materials using three-dimensional (3D) printing and shows rapid degradation by commonly found bacteria under ambient conditions.

The eco-sustainability of the 3D printable LZC is based on the principle of benign by design.[21,22] The precursors of the LZC blend are plant-based polymers that degrade into their molecular subunits when released into the environment.[23] We combine lignin and zein to produce a composite ink that can be used to 3D print materials via nozzle extrusion. Zein is a protein present in corn and is widely available as a waste product from the biofuel industry. It is an excellent candidate to replace synthetic thermoplastics in film casting and

Received: October 28, 2020
Revised: December 13, 2020
Published: January 16, 2021

© 2021 American Chemical Society

https://dx.doi.org/10.1021/acssuschemeng.0c07915
ACS Sustainable Chem. Eng. 2021, 9, 1781–1789

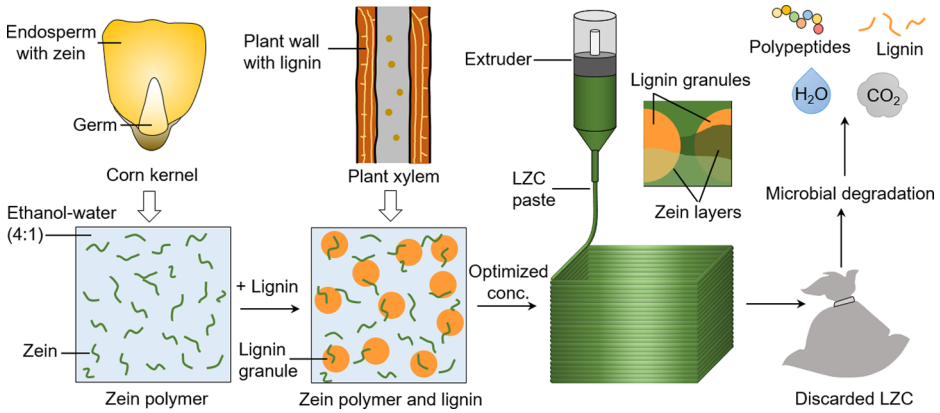

Figure 1. Scheme representing the synthesis, printing, and degradation of the LZC. Zein is dissolved in an ethanol–water (4:1) mixture at its saturation concentration. Dealkaline lignin is then dispersed in a zein solution at a concentration higher than its solubility limit to ensure lignin exists in a granular state. This LZC blend is printed into desired 3D structures using extrusion printing. After printing, solvent evaporation drives a spontaneous phase separation causing zein molecules to precipitate on the surface of lignin granules. This phase separation of zein under ambient conditions leads to the hardening of the printed structure. The LZC can be fully degraded upon exposure to the model bacteria under ambient conditions.

extrusion printing.[24,25] However, the lack of processability using 3D printers, brittle nature, and low tensile strength of the isolated zein protein limits its applicability as a viable alternative to thermoplastics.[26] We overcome these limitations by using granular lignin as a binder, which not only enhances the strength of the LZC but also enables its 3D printability. Lignin is a naturally occurring bio-polymer and is a major structural component of terrestrial plants, providing rigidity and strength to their cell walls.[27−30] It is regarded as one of the most abundant organic materials and available as a byproduct of the paper industry.[31−33]

LZCs have been synthesized previously and used as insulators and fire retardant materials.[26,34,35] However, previous methods require high-energy processing of the composite using a hot press, and the material is not transformable/processable by conventional extrusion 3D printers. In this article, we overcome these limitations by developing a new method for in-solution processing of the composite using the spontaneous change in solubility of zein in an ethanol–water mixture and its corresponding phase separation and condensation on granular lignin. We demonstrate the formation of a 3D printable ink obtained by directing the solubility and co-precipitation of lignin and zein in an ethanol–water mixture. We describe the molecular interaction between zein and lignin that leads to the condensation of zein molecules on lignin granules, which drives the change in rheological properties of the LZC ink during the drying process. We investigate the effect of relative concentration of the zein and lignin on the viscoelastic properties of the LZC and discuss the molecular origin of the enhanced mechanical strength and processability of the composite. We demonstrate the versatility of the LZC as a 3D printable ink by manufacturing various model macroscopic structures. Furthermore, we quantify the degradation of the LZC in the presence of *Sphingomonas paucimobilis* and *Stenotrophomonas maltophilia*, commonly found bacteria at waste disposal sites.[36,37]

MATERIALS AND METHODS

LZC Ink Preparation and 3D Printing. Zein powder (Acros Organics) was dissolved in a 4:1 mixture of absolute ethanol and water by sonication. Then, granular dealkaline lignin (Tokyo Chemical Industry Co., Ltd.) was dispersed in zein solution by mixing with a spatula. The ink was sonicated for ∼1 h, and the uniform distribution of lignin granules in the zein matrix was confirmed with fluorescence microscopy imaging. The concentration of dealkaline lignin was higher than its solubility limit in the aqueous mixture and thus the mixture is oversaturated with lignin. With an optimized concentration of lignin, the paste can be transformed from a honey-like zein solution to a clay-like lignin–zein composite, which is preferred in extrusion 3D printing. The composite ink was then transferred to a commercial printer (Culture 3D Tissue Scribe) to 3D print desired structures. The 3D printing was performed through a 410 μm inner diameter nozzle and printing speed of 1.0 mm s^{-1} at 25 °C and 42 % relative humidity. The printing speed was selected to achieve practical ink density for printing. At a lower speed, the dried ink was found to clog the nozzle, while at a higher speed, the extruded ink formed a discontinuous structure. All experiments were performed with ultrapure water of resistivity 18.2 MΩ cm.

Material Characterization. A Leica DM6 upright microscope equipped with a Leica DFC9000 GTC camera and a Leica EL 6000 fluorescence light source was used for imaging the dried filamentous structures in brightfield and fluorescence modes. The drying process and the zein shell formation on lignin were visualized at 25 °C on the light microscope. Scanning electron microscopy (SEM) (JEOL JSM-6610LV, 5 kV operating voltage) was used to visualize the microstructure of the printed lignin–zein composite at higher resolution. All the samples for SEM were dried at 25 °C and coated with platinum to minimize charging effects during the imaging.

Rheometry. Composite paste samples for oscillating rheometry with a fixed concentration of lignin or zein were prepared as described above. The TA Discovery HR-2 rheometer was used for oscillating rheometry with 25 mm parallel plates. Sample heights were in the range of 900–1000 μm. Storage (G') and loss (G'') moduli and tan δ of composite samples were recorded by time sweeping from 0 to 30 min immediately after mixing to demonstrate the drying process of each sample. Oscillating frequency was fixed at 1 Hz, and strain was at 10%.

Tensile Strength. A dog-bone shape was used on a tensile tester (Instron Mechanical Test System 5696) equipped with a 50 N load cell to evaluate the tensile strength of the printed structure. Maximum stress, tensile modulus, and elongation at break were measured at a strain rate of 0.50 mm min^{-1}.

Biodegradation. Sheet samples printed from acrylonitrile butadiene styrene (ABS), PLA, and LZC (c_{zein} = 1.0 g mL^{-1} and c_{lignin} = 0.6 g mL^{-1}) were used in biodegradation tests. The printed sheets with a dimension of 30 mm × 15 mm × 1 mm were kept in 15 mL of minimal media solution (composition of media solution:

https://dx.doi.org/10.1021/acssuschemeng.0c07915
ACS Sustainable Chem. Eng. 2021, 9, 1781−1789

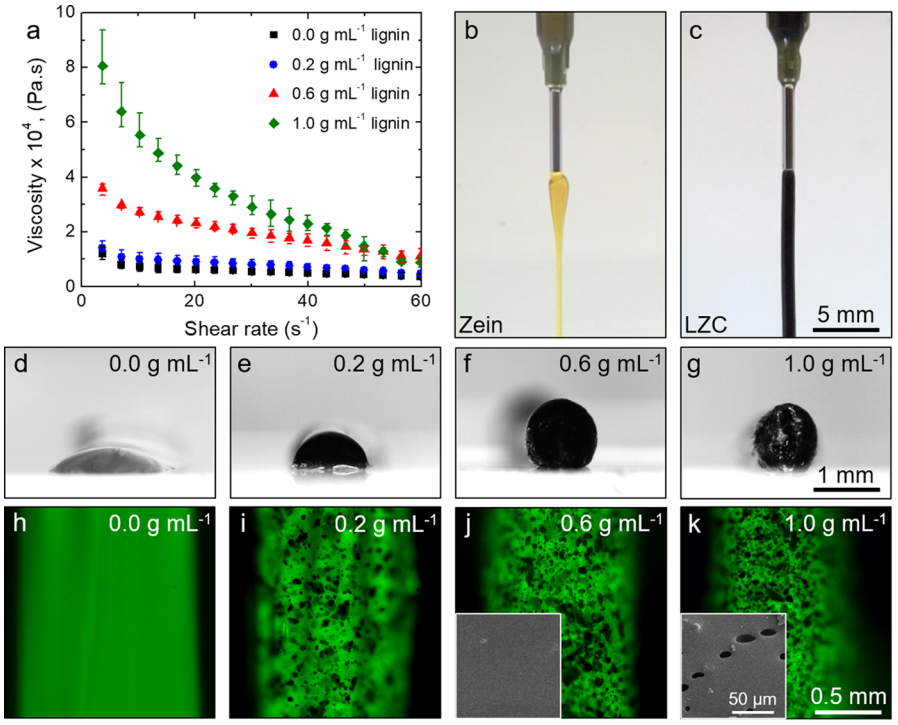

Figure 2. Extrudability and structural characteristics of LZC. (a) Complex viscosity of the zein solution and LZC blend at an increasing concentration of lignin. The blend transitions from a Newtonian fluid at low lignin concentrations to a non-Newtonian shear-thinning fluid upon adding lignin granules. (b, c) Images showing extrudability of LZC paste with lignin granules. c_{zein} is fixed at 1.0 g mL^{-1} while c_{lignin} is 0.0 g mL^{-1} in (b) and 0.6 g mL^{-1} in (c). (d–g) Images showing improved structural preservation with added lignin granules. (h–k) Fluorescence microscopy images showing a printed filament of zein and LZC with increasing c_{lignin} from 0.0 to 1.0 g mL^{-1} at fixed c_{zein} = 1.0 g mL^{-1}. Here, zein is labeled with FITC and appears green in fluorescent images. The lignin granules can be distinguished as dark aggregates within the filament. As the lignin concentration in the LZC blend increases, lignin granules are more evenly distributed in the composite. The inset SEM images in (j) and (k) show the appearance of microvoids upon increasing c_{lignin} to 1.0 g mL^{-1}, driving an increase in surface roughness shown in (g).

K_2HPO_4 (2.34 g L^{-1}), KH_2PO_4 (1.33 g L^{-1}), $MgSO_4{\cdot}7H_2O$ (0.20 g L^{-1}), $(NH_4)_2SO_4$ (1.00 g L^{-1}), NaCl (0.50 g L^{-1}), $CoCl_2$ (0.0019 mg L^{-1}), $NiCl_2$ (0.0118 mg L^{-1}), $CrCl_2$ (0.0063 mg L^{-1}), $CuSO_4$ (0.0157 mg L^{-1}), $FeCl_3$ (0.9700 mg L^{-1}), $CaCl_2$ (0.7800 mg L^{-1}), and $MnCl_2$ (0.0100 mg L^{-1}) dissolved in deionized water at pH = 7).[38] After autoclaving the sheet samples, *S. paucimobilis* (ATCC 29837) and *S. maltophilia* (ATCC 13636) (MicroBioLogics) were inoculated respectively to the samples to test their biodegradability in the presence of selected microorganisms. The inoculum was grown in a nutrient broth for 24 h before inoculation to ensure that the microorganism was in the log phase of growth, and an inoculum (0.1 mL) was placed in each vial except the controls of each composite. Printed ABS, PLA, and LZC sheets were prepared in the same manner to serve as comparison in this experiment. Triplicates of all composites and bacteria were prepared. A 90-day biodegradation test was performed after inoculation at 30 °C under ambient pressure. Images were taken using a digital camera to visualize the degradation process of each sample. At the end of 90 days, the samples were filtered through a Buchner funnel fitted with a filter paper to collect residue of the composite. The remaining structures were allowed to dry to obtain the final weight of each sample.

RESULTS AND DISCUSSION

Effect of Lignin Concentration on Viscoelasticity of the LZC. Programming the solubility of zein and lignin in the water–ethanol mixture enables the formation of a composite blend that can be processed using extrusion 3D printing. The schematic representation from the preparation of 3D printable paste to bacterial degradation of the product is summarized in Figure 1. First, zein is dissolved in a 4:1 volume ratio of the ethanol–water mixture such that the final concentration of zein is at its solubility limit (c^*_{zein}= ∼1.0 g mL^{-1}).[39] Then, 0.1–1.0 g mL^{-1} of dealkaline lignin (average diameter = 30 μm, Figure S1) is added to the zein solution, and a homogeneous blend is obtained by mixing. Note that the solubility limit of dealkaline lignin in the ethanol–water 4:1 mixture is low (c^*_{lignin} = 0.04 g mL^{-1}), thus most of the added lignin in the solution exists in an undissolved granular state (Figure S2).

The printability of an ink is governed by a complex interplay among printing parameters and rheological properties of the ink.[40] For effective extrusion printing, an ink must exhibit shear-thinning properties such that it can be extruded as a liquid at high shear rates yet be self-standing after extrusion.[41,42] The viscoelasticity of the LZC blend is tuned by the amount of added granular lignin. We investigated the effect of lignin granules on the printability of the ink by measuring the change in viscosity of the blend with an increasing lignin concentration (c_{lignin}) from 0.0 to 1.0 g mL^{-1} and a fixed concentration of zein (c_{zein}) at 1.0 g mL^{-1} (Figure 2a). In general, the viscosity of the blend increases upon adding lignin granules into the zein solution. In the absence of lignin, the viscosity of the zein solution is lower than the LZC blend and remains almost constant with the increasing shear rate in traditional Newtonian fashion.[43] As c_{lignin} increases, the viscosity at low shear rates increases, and the ink shows a shear-thinning (or pseudoplastic) behavior.[44] This transition from a near-Newtonian to a shear-thinning fluid upon adding lignin granules is attributed to the viscous force affecting the suspension structure at a high shear rate.[45] At a low shear rate, lignin granules are irregularly ordered and form aggregated

https://dx.doi.org/10.1021/acssuschemeng.0c07915
ACS Sustainable Chem. Eng. 2021, 9, 1781–1789

structures. As the shear rate increases, the aggregated structures break down into the dispersed lignin granules, which decreases the particle−particle interactions in the blend, resulting in free space between lignin granules and a decrease in viscosity.[46] Such shear-thinning behavior of the blend enables easy extrusion but prevents the collapse of printed objects, thus enhancing structural fidelity.[40,47] The improved extrudability and printability of zein upon adding lignin granules are visualized by comparing the extrusion of the zein solution and LZC blend from a nozzle (Figure 2b,c and Movie S1). The zein solution flows freely due to its low-viscosity liquid-like Newtonian response, but the LZC blend behaves as a high-viscosity liquid upon extrusion, i.e., shearing and shows solid-like non-Newtonian response after extrusion, which enables layer-by-layer printing (Figure S3).

To demonstrate the role of lignin in enhancing viscoelasticity, we compare LZC filaments printed using a nozzle of diameter 1.6 mm. Here, the c_{zein} was kept constant at 1.0 g mL^{-1}, and the c_{lignin} was gradually increased from 0.0 to 1.0 g mL^{-1}. In the absence of lignin, the zein solution spreads on the glass substrate, which highlights its fluid nature.[48] The spreading of the paste on the substrate decreases with the addition of lignin granules, and filaments extruded by c_{lignin} = 0.6 g mL^{-1} retain their "filamentous" form (Figure 2d−g). Note that c_{lignin} > 0.6 g mL^{-1} leads to sintering of lignin granules, which clog the nozzle (at a fixed extrusion pressure), making the LZC impractical for 3D printing purposes. The bulk configuration of the filament is visualized by fluorescence microscopy where the zein is labeled with fluorescein isothiocyanate (FITC) and appears green, and lignins are non-fluorescent and appear black. The fluorescence images show that micron-sized lignin granules are homogeneously distributed in the zein matrix at c_{lignin} > 0.6 g mL^{-1} (Figure 2h−k). Scanning electron microscopy (SEM) images (Figure 2j−k) show a smooth surface of LZC filaments with no significant irregularities, except for c_{lignin} = 1.0 g mL^{-1} where microvoids are observed. Based on SEM image analysis, we find that the void density on the LZC surface is ∼400 voids per mm^2 with an average diameter of ∼10 μm (Figure S4). These voids can be attributed to the decrease in the relative amount of zein in the composite, which drives the coagulation of lignin granules in a printed LZC structure[49] and deteriorates its tensile strength (discussed later).

Phase Separation of Zein and Self-Curing of the LZC. The extruded LZC object requires drying under ambient conditions, which results in the self-curing of the material by precipitation of the zein polymer onto the lignin granules. This enables interlinking of lignin granules and turns the printed viscoelastic material into a rigid structure. The solubility of zein is strongly dependent on the fraction of ethanol present in the solvent. While pure water is a poor solvent for zein, the ethanol−water mixture (4:1) dissolves zein.[50] We take advantage of this characteristic property of zein to translate a printed material into rigid objects. After the initial extrusion, the printed structure is allowed to dry for 30 min at room temperature. During this drying period, the ethanol selectively evaporates because of its higher vapor pressure, and zein precipitates to form a shell on the surface of lignin granules as shown in Figure 3a−d and Figure S5. The shell formation is the result of hydrogen bonding between hydroxyl groups on lignin and amino acids on the zein molecule.[51,52] The experiments shown in Figure 3b,c were performed at c_{zein} = 0.2 g mL^{-1}, which is insufficient to form a continuous matrix in

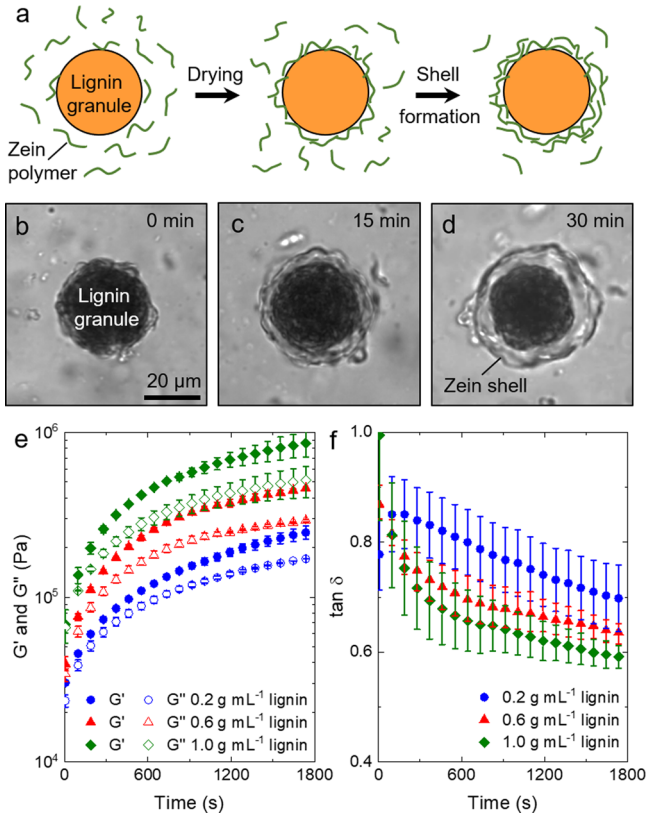

Figure 3. Condensation of zein on lignin granules and self-curing of the LZC. (a) Schematic representation of the drying process of lignin granules in a zein polymer solution. Initially, zein polymer binds to a lignin granule due to the hydrogen bonding between lignin and zein. As the drying continues, the evaporation of solvent drives the precipitation of zein and leads to the formation of a zein shell around a lignin granule. (b−d) Optical microscopy images of a lignin granule in c_{zein} = 0.2 g mL^{-1} after 0, 15, and 30 min of the drying process at 25 °C. As the mixture of zein solution and lignin granules dries, phase separation and precipitation of zein on lignin granules drive the formation of a rigid LZC structure. (e) Change in storage (G') and loss (G'') moduli of LZC paste over time with increasing c_{lignin} at c_{zein} = 1.0 g mL^{-1}. The increase in both G' and G'' demonstrates the enhancement in viscoelastic properties of the composite with the increasing concentration of lignin. (f) Change in tan δ of LZC paste over time. The decrease in tan δ upon increasing the lignin concentration indicates a solid-like behavior of the LZC in the presence of large amount of lignin granules.

the solvent bulk. As the drying proceeds at c_{zein} = 0.2 g mL^{-1}, the zein forms a continuous matrix around the lignin granules, which "solidifies" the printed structure.[48] Note that the initial zein shell formation on lignin granules is pre-bulk phase separation of zein on the high-energy lignin−solvent interface, which is followed by the bulk phase separation of zein and corresponding matrix formation.[53] We acknowledge that a small fraction of solubilized lignin in the bulk phase may interact with zein and lignin granules, thus altering the interfacial interactions. A separate study would be necessary to quantify the impact of soluble lignin on the interaction between lignin granules and zein polymer.

The drying of LZC induces a gradual increase in the "rigidity" of the printed structure. The novelty of applying the lignin−zein composite is attributed to shear thinning and the long-term stability of the composite with the evaporation of solvent, which conferred enough in-service stiffness. We

https://dx.doi.org/10.1021/acssuschemeng.0c07915
ACS Sustainable Chem. Eng. 2021, 9, 1781−1789

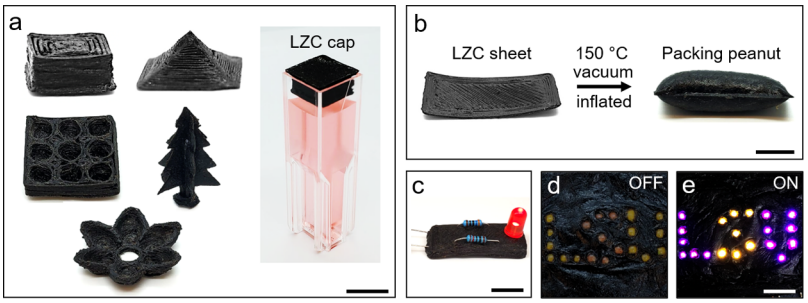

Figure 4. Examples of 3D printed structures using LZC. (a) Model 3D structures printed using the LZC demonstrating the versatility of the ink. The LZC blend used for the printing contained c_{zein} = 1.0 g mL^{-1} and c_{lignin} = 0.6 g mL^{-1} in an ethanol−water mixture. (b) Packing peanut prepared by an inflating an LZC sheet at the glass transition temperature of zein (∼150 °C) in vacuum. The sheet structure shown in (b) is used as a model structure in biodegradability tests. (c) Light-emitting diode embedded in the LZC. (d, e) Circuit board with embedded electronic components for lighting in an external power OFF and ON state. All structures were printed through a 410 μm inner diameter nozzle and printing speed of 1.0 mm s^{-1}. Scale bars = 1 cm.

quantify the change in properties of the LZC by performing oscillatory time-sweep rheometry at 25 °C for 30 min. The change in storage (G') and loss (G'') moduli of the LZC over time for c_{zein} = 1.0 g mL^{-1} and increasing c_{lignin} is shown in Figure 3e. We find that for all lignin concentrations, G' is higher than G'', indicating that all of the composites behave as solid-like viscoelastic materials.[54] All formulations exhibited a gradual increase in both storage and loss moduli over time and reached a plateau after 30 min, indicating the hardening of the LZC during the drying process. This was further quantified by determining tan δ, which is defined as the ratio of the loss-to-storage moduli, i.e., tan δ = G″/G′. tan δ is a measure of viscoelasticity of the material where tan $\delta \gg 1$ represents viscous behavior and tan $\delta \ll 0.1$ represents elastic behavior. At all tested lignin concentrations, tan δ shows a steady decrease from ∼1 as the drying proceeds, highlighting the transition of the LZC from a fluid-like state to an elastic solid-like material (Figure 3f). The tan δ values of LZC with c_{zein} = 1.0 g mL^{-1} in the nearly dried state after 30 min show a decrease with increasing c_{lignin}. Note that increasing c_{zein} at c_{lignin} = 0.6 g mL^{-1} also changes the property of the LZC blend from a liquid to a solid-like viscoelastic material (Figure S6). However, increasing c_{zein} over 1.0 g mL^{-1} impedes the nozzle extrusion process by requiring significantly higher pressures, which is undesirable for practical reasons.

We find that the mechanical strength of the printed LZC can be further improved by increasing the concentration of lignin in the composite. After the composite is printed and ethanol is completely evaporated beyond 1800 s, solid-like materials can be assessed better with a tensile method than rheometry. Thus, we quantify the change in mechanical properties of a completely dried LZC upon increasing the lignin concentration by measuring the stress−strain relationship using the Instron Mechanical Test System 5696. We print a dog-bone shape using the LZC and measure the stress versus strain relationship for LZCs with increasing c_{lignin} from 0.0 to 1.0 g mL^{-1} at c_{zein} = 1.0 g mL^{-1} (Figure S7). We find that the maximum tensile strength increases from 3.1 to 3.9 MPa as c_{lignin} increases from 0.0 to 0.6 g mL^{-1}, which is similar to the reported tensile strength of a thermoplastic zein and alkaline lignin-based nanocomposite.[34] The tensile modulus monotonically increases for c_{lignin} from 0.0 to 0.6 g mL^{-1} of lignin and decreases upon further increasing c_{lignin} (Table S1). At c_{lignin} > 0.6 g mL^{-1}, the aggregated lignin granules form microvoids, which deteriorate the mechanical rigidity of the LZCs.[55] We acknowledge that the tensile strength of the printed material is lower than that of traditional petroleum-oil based plastics.[56] Here, our aim is to present a new design principle for an inexpensive, degradable, and 3D printable bio-based plastic, and further studies are necessary for improving its mechanical properties.

Extrusion Printing of the LZC. The applicability of LZC as an ink was demonstrated by printing 3D objects using its optimized composition of c_{zein} = 1.0 g mL^{-1} and c_{lignin} = 0.6 g mL^{-1} in an ethanol−water mixture (weight percent of lignin in the ink = 25%) at a printing speed of 1.0 mm s^{-1}. A few examples of printed structures are shown in Figure 4a. The sample structures include a multicore cube, pyramid, multi-well vial holder, cuvette cap, tree, flower, sheet, and circuit boards with embedded electronic components such as light emitting diodes and resistors (Figure 4b−d). The resolution of the printed structure is governed by the diameter of the nozzle used in the printing process. The applicability of the printed shapes and objects hinges on the physical properties of the printed material. Above the glass transition temperature of zein ($T_g \approx$ 150 °C), the LZC is easily inflated in vacuum. At T_g, the precipitated zein on lignin granules is softened, and a pressure differential rapidly expands 3D-printed objects into hollow structures.[57] For example, the LZC sheet above T_g in vacuum transforms its shape into a low-density pillow-like structure, which can be used as a packing filler (Figure 4b). We also find that the printed LZC is an insulator and is stable at elevated temperatures up to 120 °C (Figure S8 and Movie S2); therefore, we anticipate that LZCs can be an alternative to non-degradable thermoplastics for manufacturing biodegradable circuit boards.[58]

Biodegradability of the LZC. The primary advantage of LZC is its rapid degradability under ambient conditions, showing its excellent environmental compatibility. Here, we perform a 90-day microbial degradation study on the LZC and two commercially used plastics, ABS and PLA. The comparative degradation was performed on a model sheet structure of identical dimension 30 mm × 15 mm × 1 mm printed using ABS, PLA, and LZC (Figure 4b). Two model bacteria capable of degrading commercial hydrocarbons were chosen for the biodegradation studies: *S. paucimobilis* and *S. maltophilia*. *S. paucimobilis* is fairly ubiquitous, routinely found in soil and water.[59,60] It can degrade a number of organic compounds including polyaromatic hydrocarbons,[61] polyhalogenated hydrocarbons,[62] and organic chloride salts.[63] *S.*

https://dx.doi.org/10.1021/acssuschemeng.0c07915
ACS Sustainable Chem. Eng. 2021, 9, 1781−1789

maltophilia can be isolated from soil, water, and human environments (e.g., hospitals).[36,64] *S. maltophilia* has been shown to degrade various hydrocarbons including PLA.[38,65] The degradation of LZC in *S. maltophilia* can be identified visually from the decomposition of the printed sheets in 90 days (Figure 5a–c), while ABS and PLA sheets retain their original shape and size (Figure 5d,e). For quantitative analysis of the biodegradation process, each sample was filtered and dried after 90 days to determine the net percentage of the weight change of each sheet (Figure 5f).

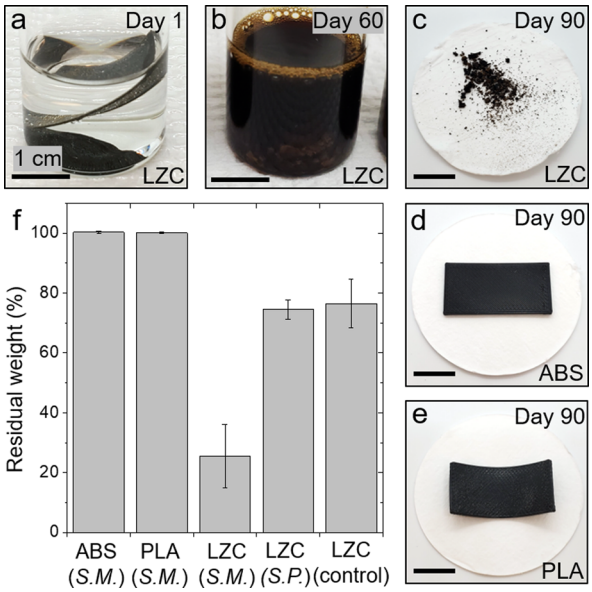

Figure 5. Biodegradation of LZC, ABS, and PLA. (a–e) Photographs from a 90-day microbial degradation study of a model sheet structure printed using (a–c) LZC, (d) ABS, and (e) PLA in aqueous media containing *S. maltophilia* under ambient conditions. The residual structures after 90 days indicate the rapid biodegradability of LZC. (f) Percentage residual weight of ABS, PLA, and LZC after 90 days of microbial degradation with bacterial culture media (control), *S. paucimobilis* (*S.P.*), and *S. maltophilia* (*S.M.*). While ABS and PLA do not exhibit any weight loss during the 90-day exposure, the LZC under *S. maltophilia* shows a significant loss of residual weight compared to culture media and *S. paucimobilis*.

The residual weight of sheets printed using ABS and PLA after a 90-day equilibration with *S. paucimobilis* or *S. maltophilia* is nearly 100%, indicating no degradation (Figure 5f). However, residual weight of the sheet structure printed using the LZC blend is ∼20% in the presence of *S. maltophilia*. For the LZC sheet in media without bacteria (control) and in the presence of *S. paucimobilis*, ∼75% of weight remains after 90 days (Figures S9 and S10). The observed change in weight of the LZC in media and *S. paucimobilis* is attributed to the increase in solubility of lignin in electrolyte solutions (culture media) due to the proton-donating ability of salts.[66,67] As a result, the lignin granules are dissolved in the bacterial culture media, which leaves the undissolved zein structure. Therefore, we find that *S. paucimobilis* is not capable of degrading zein under tested conditions. *S. maltophilia*, on the other hand, demonstrated robust LZC degradation capability under described conditions. The degradation appears to occur via two simultaneously occurring processes: (1) lignin granules in the zein matrix dissolve in the high ionic strength media, and (2) *S. maltophilia* degrades the zein structure into simple molecules such as carbon dioxide, water, and peptides.[64,68] During microbial degradation of zein by *S. maltophilia*, the quaternary and tertiary structures of the zein protein expose ionizable polar amino acids containing NH^{3+} and COO^{-} such as glutamate.[69] Thus, the enhanced water–protein interaction and electrostatic repulsion between peptides increase the water solubility of the LZC.[69] The superior biodegradability of LZC over other synthetic plastics in ambient condition demonstrates its potential in serving as an eco-friendly replacement of synthetic plastics in the manufacturing industry. At the end of their lifecycle, the structures printed from the LZC can be discarded in the environment to be naturally degraded.

CONCLUSIONS

In this work, we presented a strategy to synthesize a new class of 3D printable, bio-based LZC, which degrades in the presence of model bacteria commonly found at waste sites. An interplay of the solubility of lignin and zein in an ethanol–water mixture allows 3D printing of complex shapes using an extrusion process. We demonstrate that in the LZC blend, lignin exists in its granular state, which imparts a shear-thinning behavior that enables extrusion 3D printing of the LZC. After extrusion, controlled evaporation of solvent drives a spontaneous phase separation and precipitation of zein on the surface of lignin granules. Here, the role of zein is to interlink the lignin granules and transform the printed structure from a viscoelastic fluid to a solid. We demonstrated the versatility of the ink to print complex 3D structures including holders, caps, and circuit boards with attached electronic components. We find that the structures printed using the LZC can be degraded to ∼20% of their initial weight within 90 days of exposure to model bacteria under ambient conditions, which is not the case for PLA and ABS. The LZC developed in this work has three advantages: (1) use of inexpensive industrial byproducts lignin and zein as precursors and benign solvents, viz., ethanol and water; (2) nozzle-extrusion properties for robust 3D printability; and (3) rapid degradability under ambient conditions. We believe that because of these advantages, the LZC provides a unique platform for developing materials requiring minimal waste treatment and recycling and thus assists in addressing the global challenge of plastic pollution.

ASSOCIATED CONTENT

Supporting Information

The Supporting Information is available free of charge at https://pubs.acs.org/doi/10.1021/acssuschemeng.0c07915.

Size distribution of lignin granules; solubility limit of lignin; demonstration of change in viscosity of the LZC blend; microvoid size distribution and surface density; fluorescence images of the zein shell; rheometry and stress–strain relationship for the LZC; electrical and electrical conductivity and thermal imaging for an LZC sheet; and bacterial degradation of ABS, PLA, and LZC (PDF)

Extrusion of zein and the LZC (MP4)

Electrical conductivity of the LZC (MP4)

AUTHOR INFORMATION

Corresponding Author

Bhuvnesh Bharti − *Cain Department of Chemical Engineering, Louisiana State University, Baton Rouge,*

https://dx.doi.org/10.1021/acssuschemeng.0c07915
ACS Sustainable Chem. Eng. 2021, 9, 1781–1789

Louisiana 70803, United States; orcid.org/0000-0001-9426-9606; Email: bbharti@lsu.edu

Authors

Jin Gyun Lee − *Cain Department of Chemical Engineering, Louisiana State University, Baton Rouge, Louisiana 70803, United States*

Yusheng Guo − *Cain Department of Chemical Engineering, Louisiana State University, Baton Rouge, Louisiana 70803, United States*

Jorge A. Belgodere − *Department of Biological Engineering, Louisiana State University, Baton Rouge, Louisiana 70803, United States*

Ahmed Al Harraq − *Cain Department of Chemical Engineering, Louisiana State University, Baton Rouge, Louisiana 70803, United States*

Aubry A. Hymel − *Cain Department of Chemical Engineering, Louisiana State University, Baton Rouge, Louisiana 70803, United States*

Amber J. Pete − *Cain Department of Chemical Engineering, Louisiana State University, Baton Rouge, Louisiana 70803, United States*

Kalliat T. Valsaraj − *Cain Department of Chemical Engineering, Louisiana State University, Baton Rouge, Louisiana 70803, United States*

Michael G. Benton − *Cain Department of Chemical Engineering, Louisiana State University, Baton Rouge, Louisiana 70803, United States*

Mary G. Miller − *Science Department, Baton Rouge Community College, Baton Rouge, Louisiana 70806, United States*

Jangwook P. Jung − *Department of Biological Engineering, Louisiana State University, Baton Rouge, Louisiana 70803, United States;* orcid.org/0000-0001-5783-4549

Complete contact information is available at: https://pubs.acs.org/10.1021/acssuschemeng.0c07915

Author Contributions

‖J.G.L. and Y.G. contributed equally to this work.

Notes

The authors declare no competing financial interest.

■ ACKNOWLEDGMENTS

Authors thank Mr. Nick Lombardo (LSU) for his assistance with the experimental setup and Dr. Dongmei Cao (LSU) for the assistance with SEM imaging. Material synthesis and printing aspects were supported by Chevron Research Innovation Funds. J.G.L. was supported by Louisiana State University under the Economic Development Assistantship program. B.B. acknowledges the financial support from NSF-CAREER (CBET-1943986).

■ REFERENCES

(1) Geyer, R.; Jambeck, J. R.; Law, K. L. Production, Use, and Fate of All Plastics Ever Made. *Sci. Adv.* **2017**, *3*, No. e1700782.

(2) The Future of Plastic. *Nat. Commun.* **2018**, *9* (), 2157, DOI: 10.1038/s41467-018-04565-2.

(3) Worm, B.; Lotze, H. K.; Jubinville, I.; Wilcox, C.; Jambeck, J. Plastic as a Persistent Marine Pollutant. *Annu. Rev. Environ. Resour.* **2017**, *42*, 1−26.

(4) Law, K. L.; Thompson, R. C. Microplastics in the Seas. *Science* **2014**, *345*, 144−145.

(5) Straub, S.; Hirsch, P. E.; Burkhardt-holm, P. Biodegradable and Petroleum-Based Microplastics Do Not Differ in Their Ingestion and Excretion but in Their Biological Effects in a Freshwater Invertebrate *Gammarus Fossarum*. *Int. J. Environ. Res. Public Health* **2017**, *14*, 774.

(6) Andrady, A. L. Microplastics in the Marine Environment. *Mar. Pollut. Bull.* **2011**, *62*, 1596−1605.

(7) Kubowicz, S.; Booth, A. M. Biodegradability of Plastics : Challenges and Misconceptions. *Environ. Sci. Technol.* **2017**, *51*, 12058−12060.

(8) Hu, L.; Chernick, M.; Lewis, A. M.; Ferguson, P. L.; Hinton, D. E. Chronic Microfiber Exposure in Adult Japanese Medaka (*Oryzias Latipes*). *PLoS One* **2020**, *15*, No. e0229962.

(9) Lau, W. W. Y.; Shiran, Y.; Bailey, R. M.; Cook, E.; Stuchtey, M. R.; Koskella, J.; Velis, C. A.; Godfrey, L.; Boucher, J.; Murphy, M. B.; Thompson, R. C.; Jankowska, E.; Castillo Castillo, A.; Pilditch, T. D.; Dixon, B.; Koerselman, L.; Kosior, E.; Favoino, E.; Gutberlet, J.; Baulch, S.; Atreya, M. E.; Fischer, D.; He, K. K.; Petit, M. M.; Sumaila, U. R.; Neil, E.; Bernhofen, M. V.; Lawrence, K.; Palardy, J. E. Evaluating Scenarios toward Zero Plastic Pollution. *Science* **2020**, *369*, 1455−1461.

(10) Xu, W.; Wang, X.; Sandler, N.; Willför, S.; Xu, C. Three-Dimensional Printing of Wood-Derived Biopolymers: A Review Focused on Biomedical Applications. *ACS Sustainable Chem. Eng.* **2018**, *6*, 5663−5680.

(11) Jung, S.; Cui, Y.; Barnes, M.; Satam, C.; Zhang, S.; Chowdhury, R. A.; Adumbumkulath, A.; Sahin, O.; Miller, C.; Sajadi, S. M.; Sassi, L. M.; Ji, Y.; Bennett, M. R.; Yu, M.; Friguglietti, J.; Merchant, F. A.; Verduzco, R.; Roy, S.; Vajtai, R.; Meredith, J. C.; Youngblood, J. P.; Koratkar, N.; Rahman, M. M.; Ajayan, P. M. Multifunctional Bio-Nanocomposite Coatings for Perishable Fruits. *Adv. Mater.* **2020**, *32*, 1908291.

(12) Mohammadinejad, R.; Karimi, S.; Iravani, S.; Varma, R. S. Plant-Derived Nanostructures: Types and Applications. *Green Chem.* **2016**, *18*, 20−52.

(13) Mahmood, H.; Moniruzzaman, M.; Yusup, S.; Welton, T. Ionic Liquids Assisted Processing of Renewable Resources for the Fabrication of Biodegradable Composite Materials. *Green Chem.* **2017**, *19*, 2051−2075.

(14) Lambert, S.; Wagner, M. Environmental Performance of Bio-Based and Biodegradable Plastics: The Road Ahead. *Chem. Soc. Rev.* **2017**, *46*, 6855−6871.

(15) Iravani, S.; Varma, R. S. Plants and Plant-Based Polymers as Scaffolds for Tissue Engineering. *Green Chem.* **2019**, *21*, 4839−4867.

(16) Drumright, R. E.; Gruber, P. R.; Henton, D. E. Polylactic Acid Technology. *Adv. Mater.* **2000**, *12*, 1841−1846.

(17) Bagheri, A. R.; Laforsch, C.; Greiner, A.; Agarwal, S. Fate of So-Called Biodegradable Polymers in Seawater and Freshwater. *Global Challenges* **2017**, *1*, 1700048.

(18) Pelegrini, K.; Donazzolo, I.; Brambilla, V.; Coulon Grisa, A. M.; Piazza, D.; Zattera, A. J.; Brandalise, R. N. Degradation of PLA and PLA in Composites with Triacetin and Buriti Fiber after 600 Days in a Simulated Marine Environment. *J. Appl. Polym. Sci.* **2016**, *133* (), DOI: 10.1002/app.43290.

(19) Qi, X.; Ren, Y.; Wang, X. New Advances in the Biodegradation of Poly(Lactic) Acid. *Int. Biodeterior. Biodegrad.* **2017**, *117*, 215−223.

(20) Terrett, O. M.; Lyczakowski, J. J.; Yu, L.; Iuga, D.; Franks, W. T.; Brown, S. P.; Dupree, R.; Dupree, P. Molecular Architecture of Softwood Revealed by Solid-State NMR. *Nat. Commun.* **2019**, *10*, 4978.

(21) Richter, A. P.; Brown, J. S.; Bharti, B.; Wang, A.; Gangwal, S.; Houck, K.; Cohen Hubal, E. A.; Paunov, V. N.; Stoyanov, S. D.; Velev, O. D. An Environmentally Benign Antimicrobial Nanoparticle Based on a Silver-Infused Lignin Core. *Nat. Nanotechnol.* **2015**, *10*, 817−823.

(22) Lee, J. G.; Larive, L. L.; Valsaraj, K. T.; Bharti, B. Binding of Lignin Nanoparticles at Oil−Water Interfaces: An Ecofriendly Alternative to Oil Spill Recovery. *ACS Appl. Mater. Interfaces* **2018**, *10*, 43282−43289.

(23) Bai, L.; Greca, L. G.; Xiang, W.; Lehtonen, J.; Huan, S.; Nugroho, R. W. N.; Tardy, B. L.; Rojas, O. J. Adsorption and Assembly of Cellulosic and Lignin Colloids at Oil/Water Interfaces. *Langmuir* **2019**, *35*, 571−588.
(24) Anderson, T. J.; Lamsal, B. P. REVIEW: Zein Extraction from Corn, Corn Products, and Coproducts and Modifications for Various Applications: A Review. *Cereal Chem.* **2011**, *88*, 159−173.
(25) Jing, L.; Wang, X.; Liu, H.; Lu, Y.; Bian, J.; Sun, J.; Huang, D. Zein Increases the Cytoaffinity and Biodegradability of Scaffolds 3D-Printed with Zein and Poly(ε-Caprolactone) Composite Ink. *ACS Appl. Mater. Interfaces* **2018**, *10*, 18551−18559.
(26) Oliviero, M.; Rizvi, R.; Verdolotti, L.; Iannace, S.; Naguib, H. E.; Di Maio, E.; Neitzert, H. C.; Landi, G. Dielectric Properties of Sustainable Nanocomposites Based on Zein Protein and Lignin for Biodegradable Insulators. *Adv. Funct. Mater.* **2017**, *27*, 1605142.
(27) Iravani, S.; Varma, R. S. Greener Synthesis of Lignin Nanoparticles and Their Applications. *Green Chem.* **2020**, *22*, 612−636.
(28) Liu, L.-Y.; Patankar, S. C.; Chandra, R. P.; Sathitsuksanoh, N.; Saddler, J. N.; Renneckar, S. Valorization of Bark Using Ethanol−Water Organosolv Treatment: Isolation and Characterization of Crude Lignin. *ACS Sustainable Chem. Eng.* **2020**, *8*, 4745−4754.
(29) Conner, C. G.; Veleva, A. N.; Paunov, V. N.; Stoyanov, S. D.; Velev, O. D. Scalable Formation of Concentrated Monodisperse Lignin Nanoparticles by Recirculation-Enhanced Flash Nanoprecipitation. *Part. Part. Syst. Charact.* **2020**, *37*, 2000122.
(30) Ragauskas, A. J.; Beckham, G. T.; Biddy, M. J.; Chandra, R.; Chen, F.; Davis, M. F.; Davison, B. H.; Dixon, R. A.; Gilna, P.; Keller, M.; Langan, P.; Naskar, A. K.; Saddler, J. N.; Tschaplinski, T. J.; Tuskan, G. A.; Wyman, C. E. Lignin Valorization: Improving Lignin Processing in the Biorefinery. *Science* **2014**, *344*, 1246843−1246843.
(31) Yiamsawas, D.; Baier, G.; Thines, E.; Landfester, K.; Wurm, F. R. Biodegradable Lignin Nanocontainers. *RSC Adv.* **2014**, *4*, 11661−11663.
(32) Calvo-Flores, F. G.; Dobado, J. A. Lignin as Renewable Raw Material. *ChemSusChem* **2010**, *3*, 1227−1235.
(33) Richter, A. P.; Bharti, B.; Armstrong, H. B.; Brown, J. S.; Plemmons, D.; Paunov, V. N.; Stoyanov, S. D.; Velev, O. D. Synthesis and Characterization of Biodegradable Lignin Nanoparticles with Tunable Surface Properties. *Langmuir* **2016**, *32*, 6468−6477.
(34) Oliviero, M.; Verdolotti, L.; Di Maio, E.; Aurilia, M.; Iannace, S. Effect of Supramolecular Structures on Thermoplastic Zein−Lignin Bionanocomposites. *J. Agric. Food Chem.* **2011**, *59*, 10062−10070.
(35) Verdolotti, L.; Oliviero, M.; Lavorgna, M.; Iannace, S.; Camino, G.; Vollaro, P.; Frache, A. On Revealing the Effect of Alkaline Lignin and Ammonium Polyphosphate Additives on Fire Retardant Properties of Sustainable Zein-Based Composites. *Polym. Degrad. Stab.* **2016**, *134*, 115−125.
(36) Brooke, J. S. *Stenotrophomonas Maltophilia*: An Emerging Global Opportunistic Pathogen. *Clin. Microbiol. Rev.* **2012**, *25*, 2−41.
(37) Sun, W.; Liu, W.; Cui, L.; Zhang, M.; Wang, B. Characterization and Identification of a Chlorine-Resistant Bacterium, *Sphingomonas* TS001, from a Model Drinking Water Distribution System. *Sci. Total Environ.* **2013**, *458-460*, 169−175.
(38) Jeon, H. J.; Kim, M. N. Biodegradation of Poly(l-Lactide) (PLA) Exposed to UV Irradiation by a Mesophilic Bacterium. *Int. Biodeterior. Biodegrad.* **2013**, *85*, 289−293.
(39) Parris, N.; Dickey, L. C. Extraction and Solubility Characteristics of Zein Proteins from Dry-Milled Corn. *J. Agric. Food Chem.* **2001**, *49*, 3757−3760.
(40) Kyle, S.; Jessop, Z. M.; Al-Sabah, A.; Whitaker, I. S. 'Printability' of Candidate Biomaterials for Extrusion Based 3D Printing: State-of-the-Art. *Adv. Healthcare Mater.* **2017**, *6*, 1700264.
(41) Roh, S.; Parekh, D. P.; Bharti, B.; Stoyanov, S. D.; Velev, O. D. 3D Printing by Multiphase Silicone/Water Capillary Inks. *Adv. Mater.* **2017**, *29*, 1701554.
(42) Nguyen, N. A.; Barnes, S. H.; Bowland, C. C.; Meek, K. M.; Littrell, K. C.; Keum, J. K.; Naskar, A. K. A Path for Lignin Valorization via Additive Manufacturing of High-Performance Sustainable Composites with Enhanced 3D Printability. *Sci. Adv.* **2018**, *4*, No. eaat4967.
(43) Dubey, N.; Ferreira, J. A.; Malda, J.; Bhaduri, S. B.; Bottino, M. C. Extracellular Matrix/Amorphous Magnesium Phosphate Bioink for 3D Bioprinting of Craniomaxillofacial Bone Tissue. *ACS Appl. Mater. Interfaces* **2020**, *12*, 23752−23763.
(44) Wang, Y.; He, X.; Bruggeman, K. F.; Gayen, B.; Tricoli, A.; Lee, W. M.; Williams, R. J.; Nisbet, D. R. Peptide Programmed Hydrogels as Safe Sanctuary Microenvironments for Cell Transplantation. *Adv. Funct. Mater.* **2020**, *30*, 1900390.
(45) Bergström, L. Shear Thinning and Shear Thickening of Concentrated Ceramic Suspensions. *Colloids Surf., A* **1998**, *133*, 151−155.
(46) Petekidis, G.; Moussaïd, A.; Pusey, P. N. Rearrangements in Hard-Sphere Glasses under Oscillatory Shear Strain. *Phys. Rev. E* **2002**, *66*, No. 051402.
(47) Nguyen, N. A.; Bowland, C. C.; Naskar, A. K. A General Method to Improve 3D-Printability and Inter-Layer Adhesion in Lignin-Based Composites. *Appl. Mater. Today* **2018**, *12*, 138−152.
(48) Koos, E.; Willenbacher, N. Capillary Forces in Suspension Rheology. *Science* **2011**, *331*, 897−900.
(49) Tripathi, A.; Rutkevičius, M.; Bose, A.; Rojas, O. J.; Khan, S. A. Experimental and Predictive Description of the Morphology of Wet-Spun Fibers. *ACS Appl. Polym. Mater.* **2019**, *1*, 1280−1290.
(50) Patel, A.; Hu, Y.; Tiwari, J. K.; Velikov, K. P. Synthesis and Characterisation of Zein−Curcumin Colloidal Particles. *Soft Matter* **2010**, *6*, 6192−6199.
(51) Huang, J.; Zhang, L.; Chen, F. Effects of Lignin as a Filler on Properties of Soy Protein Plastics. I. Lignosulfonate. *J. Appl. Polym. Sci.* **2003**, *88*, 3284−3290.
(52) Baumberger, S.; Lapierre, C.; Monties, B.; Valle, G. D. Use of Kraft Lignin as Filler for Starch Films. *Polym. Degrad. Stab.* **1998**, *59*, 273−277.
(53) Bharti, B.; Fameau, A. L.; Rubinstein, M.; Velev, O. D. Nanocapillarity-Mediated Magnetic Assembly of Nanoparticles into Ultraflexible Filaments and Reconfigurable Networks. *Nat. Mater.* **2015**, *14*, 1104−1109.
(54) Aramaki, K.; Koitani, S.; Takimoto, E.; Kondo, M.; Stubenrauch, C. Hydrogelation with a Water-Insoluble Organogelator − Surfactant Mediated Gelation (SMG). *Soft Matter* **2019**, *15*, 8896−8904.
(55) Satam, C. C.; Irvin, C. W.; Coffey, C. J.; Geran, R. K.; Ibarra-Rivera, R.; Shofner, M. L.; Meredith, J. C. Controlling Barrier and Mechanical Properties of Cellulose Nanocrystals by Blending with Chitin Nanofibers. *Biomacromolecules* **2019**, *21*, 545−555.
(56) Tanikella, N. G.; Wittbrodt, B.; Pearce, J. M. Tensile Strength of Commercial Polymer Materials for Fused Filament Fabrication 3D Printing. *Addit. Manuf.* **2017**, *15*, 40−47.
(57) Madeka, H.; Kokini, J. L. Effect of Glass Transition and Cross-Linking on Rheological Properties of Zein: Development of a Preliminary State Diagram. *Cereal Chem.* **1996**, *73*, 433−438.
(58) Irimia-Vladu, M. "Green" Electronics: Biodegradable and Biocompatible Materials and Devices for Sustainable Future. *Chem. Soc. Rev.* **2014**, *43*, 588−610.
(59) Peng, X.; Egashira, T.; Hanashiro, K.; Masai, E.; Nishikawa, S.; Katayama, Y.; Kimbara, K.; Fukuda, M. Cloning of a *Sphingomonas Paucimobilis* SYK-6 Gene Encoding a Novel Oxygenase That Cleaves Lignin-Related Biphenyl and Characterization of the Enzyme. *Appl. Environ. Microbiol.* **1998**, *64*, 2520−2527.
(60) Perola, O.; Nousiainen, T.; Suomalainen, S.; Aukee, S.; Kärkkäinen, U.-M.; Kauppinen, J.; Ojanen, T.; Katila, M.-L. Recurrent *Sphingomonas Paucimobilis* -Bacteraemia Associated with a Multi-Bacterial Water-Borne Epidemic among Neutropenic Patients. *J. Hosp. Infect.* **2002**, *50*, 196−201.
(61) Ye, D.; Siddiqi, M. A.; Maccubbin, A. E.; Kumar, S.; Sikka, H. C. Degradation of Polynuclear Aromatic Hydrocarbons by *Sphingomonas Paucimobilis*. *Environ. Sci. Technol.* **1996**, *30*, 136−142.
(62) Nishiyama, M. Identification of Soil Micro-Habitats for Growth, Death and Survival of a Bacterium, γ-1,2,3,4,5,6-Hexachlor-

https://dx.doi.org/10.1021/acssuschemeng.0c07915
ACS Sustainable Chem. Eng. 2021, 9, 1781−1789

ocyclohexane-Assimilating *Sphingomonas Paucimobilis*, by Fractionation of Soil. *FEMS Microbiol. Lett.* **1992**, *101*, 145−150.
(63) Ayed, L.; Chaieb, K.; Cheref, A.; Bakhrouf, A. Biodegradation of Triphenylmethane Dye Malachite Green by *Sphingomonas Paucimobilis*. *World J. Microbiol. Biotechnol.* **2009**, *25*, 705−711.
(64) Miyaji, T.; Otta, Y.; Shibata, T.; Mitsui, K.; Nakagawa, T.; Watanabe, T.; Niimura, Y.; Tomizuka, N. Purification and Characterization of Extracellular Alkaline Serine Protease from *Stenotrophomonas Maltophilia* Strain S-1. *Lett. Appl. Microbiol.* **2005**, *41*, 253−257.
(65) Urszula, G.; Izabela, G.; Danuta, W.; Sylwia, Ł. Isolation and Characterization of a Novel Strain of Stenotrophomonas Maltophilia Possessing Various Dioxygenases for Monocyclic Hydrocarbon Degradation. *Braz. J. Microbiol.* **2009**, *40*, 285−291.
(66) Akiba, T.; Tsurumaki, A.; Ohno, H. Induction of Lignin Solubility for a Series of Polar Ionic Liquids by the Addition of a Small Amount of Water. *Green Chem.* **2017**, *19*, 2260−2265.
(67) Ajdary, R.; Tardy, B. L.; Mattos, B. D.; Bai, L.; Rojas, O. J. Plant Nanomaterials and Inspiration from Nature: Water Interactions and Hierarchically Structured Hydrogels. *Adv. Mater.* **2020**, *2001085*, 2001085.
(68) Verdolotti, L.; Lavorgna, M.; Oliviero, M.; Sorrentino, A.; Iozzino, V.; Buonocore, G.; Iannace, S. Functional Zein−Siloxane Bio-Hybrids. *ACS Sustainable Chem. Eng.* **2014**, *2*, 254−263.
(69) Kong, B.; Xiong, Y. L. Antioxidant Activity of Zein Hydrolysates in a Liposome System and the Possible Mode of Action. *J. Agric. Food Chem.* **2006**, *54*, 6059−6068.

https://dx.doi.org/10.1021/acssuschemeng.0c07915
ACS Sustainable Chem. Eng. 2021, 9, 1781−1789